Carbohydrate Polymer Technologies and Applications 5 (2023) 100276

Contents lists available at ScienceDirect

Carbohydrate Polymer Technologies and Applications

journal homepage: www.sciencedirect.com/journal/carbohydrate-polymer-technologies-and-applications

Effectiveness of alkaline and hydrothermal treatments on cellulosic fibers extracted from the Moroccan *Pennisetum Alopecuroides* plant: Chemical and morphological characterization

Hicham Elmoudnia [a,*], Paulina Faria [b], Rachid Jalal [a], Mohamed Waqif [a], Latifa Saadi [a]

[a] Department of Chemistry, Faculty of Sciences and Technology, Cadi Ayyad University, Marrakech, Morocco
[b] CERIS, Department of Civil Engineering, NOVA School of Science and Technology, NOVA University of Lisbon, Lisbon, Portugal

ARTICLE INFO

Keywords:
Surface properties
Alkaline treatment_hydrophobic treatment
Vegetal fibers
Fiber characterization

ABSTRACT

This work aims to study the physical, chemical, and thermal properties of natural fibers extracted from the *Pennisetum alopecuroides* plant. The study was carried out on raw and treated fibers to assess improvements that facilitate future uses in composites. The alkaline treatment was carried out using NaOH with different concentrations (1, 3, 5, and 10%) for 2 hours. Hydrothermal treatment was performed at different immersion times in a water bath at 100°C. The chemical composition of *Pennisetum alopecuroides* fibers, such as cellulose, hemicellulose, lignin, and ash contents, was evaluated. The structure of the fiber was analyzed by FTIR, SEM, and X-ray diffraction. Thermogravimetric analysis (TGA) is used to study the thermal stability of the fiber. The density was also investigated with the pycnometric methode. The results showed that a concentration of 3% NaOH during the 2h is the most suitable solution to treat the *P.alopecuroides* fiber, but the hydrothermal treatment for 1h at 100°C is also effective for this fiber. The treated fibers seem viable to be used as reinforcement for composites production, namely to achieve goals of energy efficiency.

1. Introduction

In recent years, the use of natural fibers as reinforcements for various materials has attracted the attention of several researchers (Khoudja et al., 2021; Omrani et al., 2020). The use of natural fibers as reinforcements in various matrices to replace commercially available synthetic fibers is mainly due to environmental factors and marginal costs (Sanjay et al., 2018).

Plant-derived natural fibers have great potential for use in the plastic, automotive, and packaging industries (Arthanarieswaran et al., 2015; Lau et al., 2018; Ravindran et al., 2020), as well as in the construction industry (Nunes et al., 2021). Depending on the fibers, they may have excellent characteristics such as low density, high specific stiffness, good mechanical properties, biodegradability, being environmentally friendly, toxicologically harmless, and contributing for good thermal and acoustic insulation (Ridzuan et al., 2016). Plant fibers are composed of celluloses, hemicelluloses, and lignin. Other components are in small amounts, such as lipids, proteinaceous materials, and mineral materials. The proportion of these components depends strongly on the species, climatic conditions, and the plant organ (Yang et al., 2007).

The main problems with the use of lignocellulosic fibers as reinforcement in mineral or organic matrices are the risk for biological colonisation (Cintura et al., 2022) and degradability, and compatibility with the matrices. Particularly the latter remains a weak point. Several treatments have been done to solve this problem to improve the compatibility of the fiber/matrix interface and thermal stability. Different chemical and physical treatments of natural fibers have been analyzed in several studies to assess the different physical-chemical properties obtained. One of the most used is the alkaline treatment, which consists of treating the plant biomass in an alkaline solution to remove lignin, hemicellulose, waxy substances, and natural oils that coat the outer surface of the fiber cell wall (Cai et al., 2015; Faruk et al., 2012). Pandiarajan et al. (2022) studied the effect of alkali treatment on *Thespesia populnea* fiber with 1% sodium hydroxide (NaOH) for a duration of 1h, showing that the crystallinity index increased from 41% to 65%. The thermal stability of the fiber was increased from 210°C for the untreated fiber to 230°C for the fiber treated with NaOH. Singh et al.

* Corresponding author at: Chemistry, Cadi Ayyad University Faculty of Science and Technology Gueliz, 112 Bd Abdelkrim Al Khattabi, Marrakech 40000, Morocco.
E-mail address: hicham.elmoudnia@ced.uca.ma (H. Elmoudnia).

https://doi.org/10.1016/j.carpta.2022.100276

Available online 16 December 2022

(2022) treated *corn leaf* fibers with NaOH solution at different concentrations ranging from 5 to 15% for 90 min at 80°C and 90°C, respectively. Fourier transform infrared spectroscopy (FTIR) results and chemical composition confirmed the removal of hemicellulose and lignin and the alkaline treatment at 15% and 90°C was considered the optimal treatment for this fiber. Umashankaran & Gopalakrishnan. (2021) conducted a study on the chemical modification of *Pongamia pinnata (L.)* fiber with 5% NaOH solution for different immersion times (15, 30, 45, 60, and 75 min). It was found that the 5% NaOH treatment for 60 min improved the crystallinity index (from 45% to 52%). The tensile strength and Young's modulus of the modified fiber increased from 322 MPa to 344 MPa, 10 GPa to 13 GPa, respectively.

Few studies deal with the extraction and characterization of fibers from *Pennisetum alopecuroides* plant for pulp and papermaking applications. El Omari et al. (2017) conducted a study in which they evaluate the properties of handsheets produced with three different types of plant fibers (*Typha, Pennisetum, and Agave*). It has been observed from the study of mechanical properties that increase in the *Agave* fraction had positive effects on the resistant to tearing of paper due to the length of fibers, which establish links with other fibers of the network, thus improving strength properties.

Pennisetum alopecuroides, is a member of the grass family (Poaceae) and is native to Africa (1913). Centuries ago, this plant was introduced as animal feed in South America, Asia, and Australia. In Morocco, this plant grows everywhere with important quantities in the cities at the roadside, and can reach heights up to 2 m. Every year the maintenance of public green spaces generates enormous quantities of *P.alopecuroides* plants which are generally rejected in the free surfaces of the city. This cellulose-rich waste could be exploited either as a base material, as reinforcement for composites, or in the elaboration of insulating materials. To the authors knowledge, no study has been conducted on the chemical, morphological and physical characterization of the Moroccan *P.alopecuroides* fiber for its application in the field of biocomposites, such has been done to other vegetal wastes (de Andrade Silva et al., 2008). It is in this perspective that the objective of this study lies.

Fibers were extracted from the harvested *P.alopecuroides* and physicochemical analysies, before and after chemical treatments, were performed to assess the effect and optimize the treatment. The aim is to improve the surface adhesion to a matrix, to increase its potential for being used as raw material for the manufacture of composites, namely insulating boards for buildings and other industries, to contribute for eco-efficiency.

2. Materials and methods

2.1. Fibers and treatments

The leaves of the *P.alopecuroides (PA)* plant used in this study were harvested after manual pruning from the green spaces of the city of Marrakech, Morocco. Afterward, the leaves were washed several times with distilled water and dried in an oven at 60°C for 24 h. They were then manually cut to a length of about 5 cm for further use.

Chemical treatments (alkaline and hydrothermal) of the prepared fibers were performed to modify the surface and prepare them to have a good adhesion to a matrix.

2.1.1. Alkaline treatment

Alkali treatment of natural fibers is expected to promote the ionization of hydroxyl groups to alcoxide which changes the chemical bonds and structure of the fiber (Ariawan et al., 2020). The treatment was performed with 1%, 3%, 5%, and 10 wt% NaOH solution, with a solution ratio of 1:25 (w/v) at room temperature for 2 h to remove hemicellulose and surface contaminants (Fig. 1). Finally, a 1 wt% acetic acid solution was used to neutralize the fibers immerging them during 5 min, followed by immersion in distilled water. The fibers were then dried in an oven at 60°C for 24 h (Indran & Raj, 2015).

2.1.2. Hydrothermal treatment

The treatment was performed according to the protocol described by Ajouguim et al. (2019). The *P. alopecuroides* fibers were immersed in

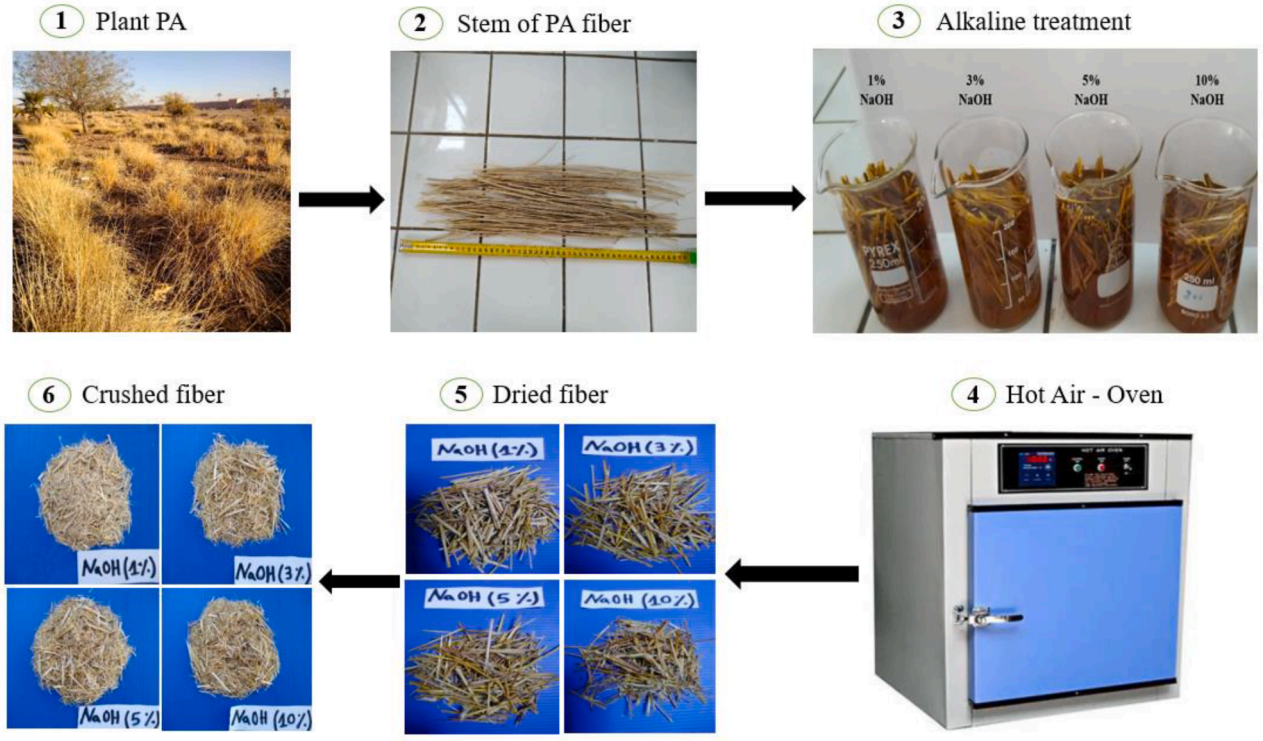

Fig. 1. *PA* fiber extraction process and after NaOH treatment: in nature, cut stem, alkaline treatment, oven dried after NaOH treatment and after being crushed.

boiling water at 100°C temperature for the different duration of 15 min, 30 min and, 60 min. The treated fibers were washed with distilled water and dried at room temperature for 48 h.

After chemical treatment, the raw and treated fibers were ground with an electric mill (Lamacom, model BL0153) before characterization.

2.2. Characterization techniques

2.2.1. Chemical analysis

2.2.1.1. Cellulose content. The cellulose content of the untreated and chemically treated fibers was analyzed by the method of Kushner and Hoffer (Sanjay et al., 2018). The fibers were soaked in a mixture of nitric acid and ethanol (HNO_3-C_2H_5OH) with a ratio of 1:4 for 4 h. The samples were then dried in an oven at 60°C to a constant weight. Cellulose content is calculated based on Eq. (1)

$$\%cellulose = \frac{W_2}{W_1} \times 100 \quad (1)$$

being W_1 the mass of the fibers before treatment and, W_2 after treatment.

2.2.1.2. Lignin content. The lignin content was estimated according to the ASTM D 1106-96 standard method. The fibers were submitted to a treatment with an ethanol-toluene mixture with a ratio of 1:2 by a soxhlet apparatus during 8h and their mass was assessed.1g of the fibers recovered after treatment with the ethanol-toluene mixture was stirred in 15 mL of a 72% sulfuric acid solution (H_2SO_4) for 2 h. Afterward, 560 mL of distilled water is added and the mixture is boiled for 4 h. After this hydrolysis, the residue is filtered by vacuum suction and then washed with 500 mL of hot water to remove all traces of acid, and oven-dried at 103±2°C for 2 h. The percentage of extracted lignin can be calculated using the Eq. (2)

$$\%lignin = \frac{W_2}{W_1} \times (100 - W_3) \quad (2)$$

being W_1 and W_2 the masses of *PA* fibers before and after treatment, and W_3 the mass obtained after the solubility test of the fibers in the ethanol-toluene mixture (%).

2.2.1.3. Hemicellulose content. Hemicellulose content was determined according to the protocol adopted by Boopathi et al. (2012). *PA* fibers were immersed in a 5% NaOH solution at room temperature for 30 min and then neutralized with HCl solution. Finally, the fibers were dried in an oven at 105°C for 2 h. The difference in weight provides the hemicellulose content by Eq. (3)

$$\%Hemicellulose = (W_1 - W_2) \times 100 \quad (3)$$

being W_1 and W_2 the masses of the fibers before and after treatment.

2.2.2. Physical analysis

2.2.2.1. Diameter and density. The diameter of the *P.alopecuroides* fibers was measured using scanning electron microscope. Five samples were examined in three distinct regions and the average diameter was reported. Density was determined following the ASTM D578-89 standard method with toluene (866 kg/m^3) as the immersion liquid. Fiber density was calculated using Eq. (4):

$$\rho_{PA} = \left(\frac{m_2 - m_1}{(m_3 - m_1) - (m_4 - m_2)}\right)\rho_{toluène} \quad (4)$$

being m_1 the mass of the empty pycnometer (g), m_2 the mass of the pycnometer filled with the *PA* fibers (g), m_3 the mass of the pycnometer filled with toluene (g) and, m_4 the mass of the pycnometer filled with the *PA* fibers and toluene (g).

2.2.2.2. Scanning electron microscopy. The morphology of *P.alopecuroides* fibers before and after treatment was examined using a JEOL JSM-5500 (VEGA3 TESCAN) scanning electron microscope equipped with an EDAX detector. To determine the atomic percentage of the present elements on the surface of the raw fiber, the energy dispersive X-ray spectroscopic technique (SEM-EDX) was used. Before analysis, all samples were coated with carbon using the sputtering technique (model 108carbon/A).

2.2.2.3. X-ray diffraction. The XRD tests were performed using a Philips X'Pert MPD diffractometer at 40 kV and 15 mA at room temperature. The anticathode was copper (Kα = 1.5418 Å). The scan angle (2θ) was between 5 and 75°. The treated and untreated fibers were placed on a stainless steel support. The crystallinity index of the *PA* fiber was calculated using the Segal method (Segal et al., 1959) (Eq. (5)):

$$I_{cr} = \frac{I_{200} - I_{am}}{I_{200}} \times 100 \quad (5)$$

being I_{200} the maximum intensity of the spectrum (amorphous or crystalline) at 2θ = 22° and I_{am} the minimum intensity of the amorphous part at 2θ = 18° (Hernandez et al., 2018).

The Scherrer's formula was used to determine the crystallite size of the *PA* fiber (Eq. (6)) (Ahmed et al., 2019).

$$Cs = \frac{k.\lambda}{\beta.\cos\theta} \quad (6)$$

being K = 0.89 the Scherrer constant, λ the wavelength of the diffracting ray (Kα1 line), β the width at half height of the peak (200) and θ the diffraction angle of the peak (200).

The numerical values are λ = 1.54184 A° and 2θ = 22.2° (French & Santiago Cintrón, 2013; Maache et al., 2017).

2.2.2.4. Fourier transform infrared (FTIR) analysis. The infrared spectra of raw and chemically treated *P.alopecuroides* were recorded using a Bruker Vertex 70 Fourier transform infrared spectrophotometer in the wavelength range 4000–400 cm^{-1}. For this purpose, 1 mg treated and untreated fibers was ground and mixed with 99 mg of KBr powder and the mixture was compressed into plates for FTIR analysis.

2.2.2.5. Thermogravimetric analysis (TGA). Thermal stability of *P.alopecuroides* fiber was ***performed*** using a Setaram Setsys 24 Discovery TGA thermogravimetric analyzer. The raw fibers were grounded and 23 mg were placed in a platinum crucible and heated in the temperature range of 25°C to 800°C at a rate of 10°C per minute under a constant flow of nitrogen, which provides an inert atmosphere during pyrolysis.

3. Results and discussion

3.1. Morphological analysis

SEM observations were conducted on the longitudinal (Fig. 2a) and transverse (Fig. 2b,c,d) sections of the raw fibers. The surface of the longitudinal section (Fig. 2a) clearly shows a layer of wax and other impurities. It justifies the need of removal of surface impurities from the fibers by proper chemical treatment to help improving fiber adhesion to a matrix.

Fig. 2b,c,d shows the cross-section of *PA* fiber, in which the lumen, microfibrils, and cell walls are observed. They are visible due to the presence of amorphous constituents like hemicellulose, lignin, and wax which help in the formation of this hollow structure. This type of morphology has been observed for other natural fibers like *Citrullus lanatus climber, Agave Americana*, and *chloris barbata* (Balasundar et al., 2018a; Khan et al., 2022; Msahli et al., 2015).

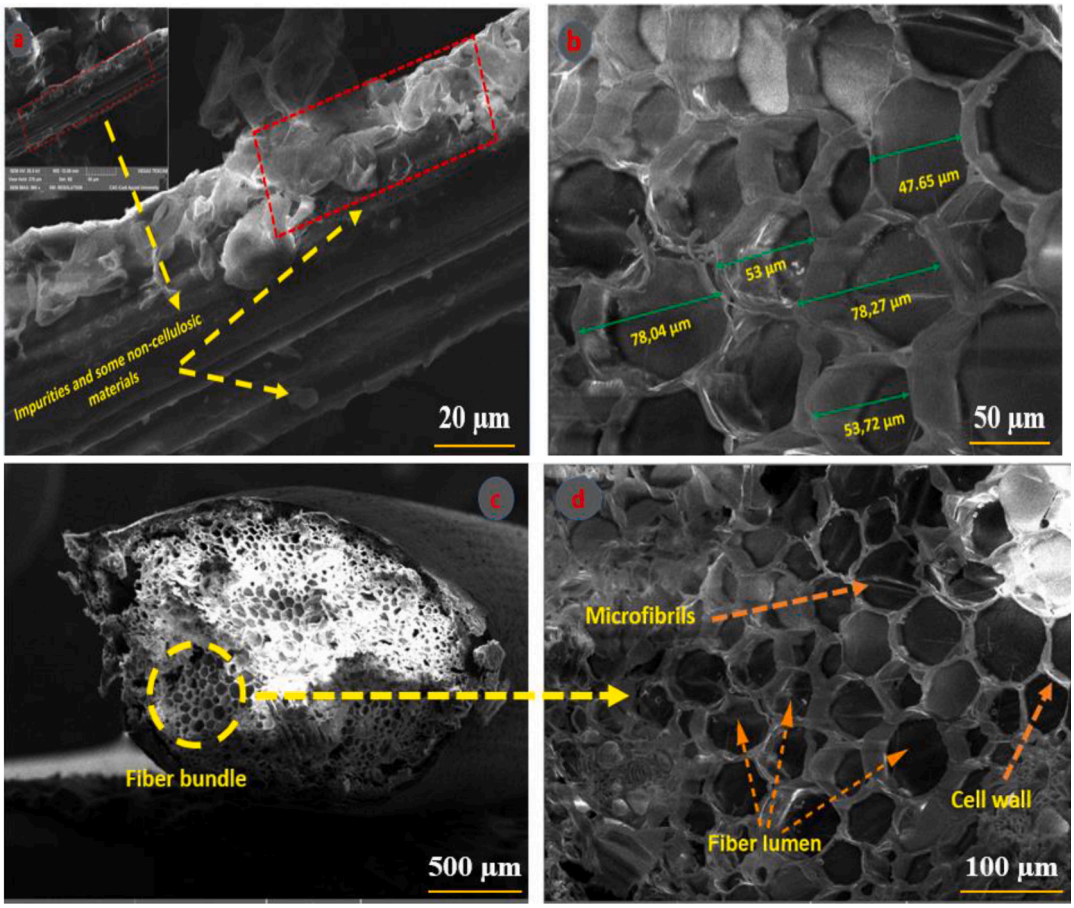

Fig. 2. SEM micrographs of the longitudinal (a) and transverse section of the raw *PA* fiber at three different magnifications: (b) higher, (c) lower, and (d) medium.

Water absorption is highly dependent on the size of the lumen. The larger the lumen and porous are the fibers structure, the easier it is for the fiber to absorb more water, and better it is to promote penetration when used as reinforcement in composites (Kamaruddin et al., 2021).

3.2. Chemical characterization

The chemical compositions of the raw (untreated) *P.alopecuroides* fibers, after alkaline treatment with 3% NaOH for 2 h at 25 °C, after hydrothermal treatment in boiling water for 60 min, and of other plant

Table 1
Physical properties and chemical composition of *PA* fibers in comparison with other natural fibers.

Fiber	Chemical properties				Physical properties		XRD		References
	Cellulose (wt.%)	Hemi cellulose (wt.%)	Lignin (wt.%)	Ash (wt.%)	Diameter (µm)	Density (g/cm^3)	CI (%)	CS (nm)	
P.alopecuroides (raw)	40	29.5	19.66	6,76	30-140	0.87	49.14	0.49	Current study
PAA3	50	23	17.5	3.42	-	-	60.02	-	Current study
PAH60	45	27.2	18.3	4.24	-	-	55.24	-	Current study
Pennisetum orientale grass	60.3	16	12.45	-	213.1	1.04	33.5	62.02	(Vijay et al., 2021)
Cissus quadrangularis stem	82.73	7.96	11.27	-	770 - 870	1.220	47.15	31.55	(Indran & Raj, 2015)
Phaseolus vulgaris	62.17	7.04	9.13	9.02	53.56	0.852	43.02	4.07	(Gurukarthik Babu et al., 2019)
Furcraea foetida	68.35	11.46	12.32	6.53	12.8	0.780	52.6	28.36	(Manimaran et al., 2018)
Chloris barbata	65.37	10.23	9.32	2.52	180-200	0.634	50.29	-	(Balasundar et al., 2018b)
Sansevieria cylindrica	79.7	10.13	3.8	-	6-30	0.915	60	86	(Kathirselvam et al., 2019)
Borassus fruit	68.94	14.03	5.37	-	241 .18	1.256	-	-	(Manimaran et al., 2019)
Agave Americana	68.42	15.67	4.85	-	126-344	1.200	-	-	(Moshi et al., 2020)
Albizia amara	64.54	14.32	15.61	4.1	-	1.043	-	-	(Senthamaraikannan et al., 2019; Senthamaraikannan & Kathiresan, 2018)
Azadiratcha indica	68.42	13.72	13.58	-	-	0.740	-	2.75	(Maheshwaran et al., 2018)
Acacia Arabica	68.1	9.36	16.86	-	-	1.028	51.72	15	(Maheshwaran et al., 2018; Manimaran et al., 2019)
Perotis indica	68.4	15.7	8.35	-	-	0.785	48.3	15	(Prithiviraj et al., 2016)
Juncus plant	40	21	29	4.41	3300	0.385	-	-	(Naili et al., 2017)

fibers from literature are presented in Table 1. The untreated *P.alopecuroides* fiber contains 40% cellulose, 29.5% hemicellulose, 19.66% lignin, 6.76% ash. The cellulose content of raw *P.alopecuroides* fiber is close to that of *Juncus effusus L* fiber (Naili et al., 2017). Raw *P.alopecuroides* fiber contains a higher amount of hemicellulose and lignin compared to *Agave Americana* (15.67% and 4.85%, respectively (Moshi et al., 2020) and *Sansevieria cylindrica* fiber (10.13% and 3.8%, respectively (Manimaran et al., 2019).

3.3. Physical characterization

The diameter of the *PA* fiber is compared to other lignocellulosic fibers, based on Table 1.

The density of the raw *PA* fibers, measured by the pycnometer method, is equal to 0.87 g.cm^{-3}. This value is relatively similar to that of *Phaseolus vulgaris* (0.852 g.cm^{-3}) and other lignocelluosic fibers when compared to literature (Table 1); this means that the *PA* fibers will be very useful for the fabrication of lightweight composites.

The low density value between natural fibers occurs due to parameters such as extraction methods, the presence of pores in the fibers, and environmental conditions (Belouadah et al., 2015; Sathishkumar et al., 2013).

3.4. Microstructural properties

3.4.1. Raw Pennisetum fibers

Fig. 3 and Fig. 4, represent the infrared spectrum and diffractometer of *P.alopecuroides* fibers in the raw state, respectively. The infrared spectrum analysis shows a band at 3430 cm^{-1} corresponding to the O-H stretching of α-cellulose (Ferreira et al., 2015; Jayaramudu et al., 2010). The two absorption bands at about 2922 cm^{-1} and 2853 cm^{-1} are attributed to the CH and CH_2 stretching vibrations of cellulose and hemicellulose (Ko et al., 2019; Sathishkumar et al., 2013). The absorption band around 1734 cm^{-1} can be attributed to the C=O carbonyl stretching absorption of the ester group or carboxyl group in hemicellulose (Bezazi et al., 2014; Morán et al., 2008; Prado & Spinacé, 2019; Reddy et al., 2014).

The significant band noted at 1639 cm^{-1} can be attributed to the aromatic ring (C=H) of lignin (Chakravarthy et al., 2020), while a small band at 1515 cm^{-1} indicates C=C stretching of the lignin aromatic ring (De Rosa et al., 2011; El Achaby et al., 2018). A band at 1460 cm^{-1} corresponds to the asymmetric bending of CH_3 in the methoxyl group (Moosavinejad et al., 2019). The peak at 1320 cm^{-1} is attributed to the C-O groups of the aromatic ring in polysaccharides (Maache et al., 2017).

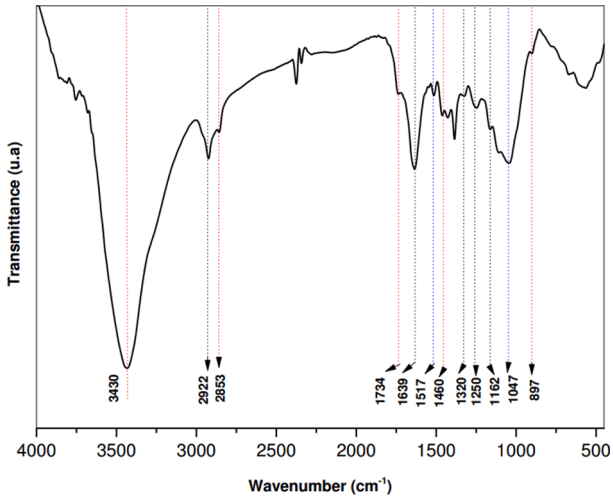

Fig. 3. FTIR spectrum of the raw *PA* fibers.

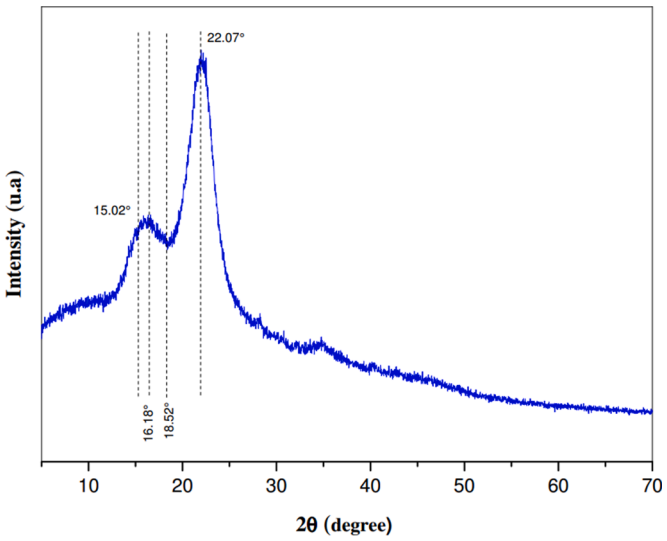

Fig. 4. X-ray diffractogram of the raw *PA* fiber.

The bands located at 1162 cm^{-1} and 1250 cm^{-1} correspond to the antisymmetric deformation of C-O-C (cellulose and hemicellulose) and the out-of-plane stretching vibration of the C-O of the aryl group, respectively (Ajouguim et al., 2019; Ibrahim et al., 2010; Saravanakumar et al., 2013).

The band at 895 cm^{-1} is associated with the C-O-C stretching vibration characteristic of β-glycosidic bonds between the anhydroglucose units of cellulose (El Achaby et al., 2018; Elanthikkal et al., 2010; Zhou et al., 2012).

3.4.2. Treated vs untreated Pennisetum fibers

Fig. 5 shows the FTIR spectra of the raw and treated *PA* fibers. The band positions and possible assignments are shown in Tables 2 and 3. The spectra are identical, except for the disappearance of the band at 1734 cm^{-1} as a result of hemicellulose removal. From the results of the two treatments, it can be inferred that the alkaline treatment provides a good removal of amorphous components than the hydrothermal treatment. In addition, the FTIR study confirmed the results on the chemical compositions of the treated and untreated *PA* fiber previously found.

X-ray diffraction analysis was performed on the *PA* fibers. From Fig. 5, we can observe major peaks are present. The first two peaks, observed at 15.02° and 16.18, correspond to the (1-10) and (110) planes respectively. This indicates the presence of amorphous components in the *PA* fiber. In addition to this, a sharp peak of high intensity observed at 22.07° corresponds to the (200) plane of cellulose I (Senthamaraikannan & Kathiresan, 2018; Vinod et al., 2021).

The crystallinity index value of *PA* fiber calculated by Segal's method is 49.14%. As shown in Table 1, the crystallinity index of raw *PA* fiber is higher than that of *Pennisetum oriental grass* (33.5%) (Vijay et al., 2021), *Phaseolus vulgaris* (43%) (Gurukarthik Babu et al., 2019) but lower than that calculated for *Sansevieria cylindrica* (60%) (Kathirselvam et al., 2019) and *Furcraea foetida* (52.6%) (Manimaran et al., 2018).

Fig. 6a and Fig. 7 show the X-ray spectra and the evolution of crystallinity of *P.alopecuroides* fibers as a function of the percentage of alkali treatment respectively. It can be observed that when the fibers were treated with alkali from 1% to 3% concentration, the crystalline cellulose content increased from 49.14% to 60.02%. This may be due to the formation of new hydrogen bonds between some cellulose chains due to the removal of hemicelluloses and lignin, which usually separate the cellulose chains. On the other hand, due to the rearrangement of crystalline regions (Reddy et al., 2014). Treatment with 3% alkali gave the best crystallinity index (60.02%). However, when treated with 5% to 10% alkali the crystalline cellulose content decreased rapidly (55.83%), indicating the polymorphic transformation to cellulose II that causes

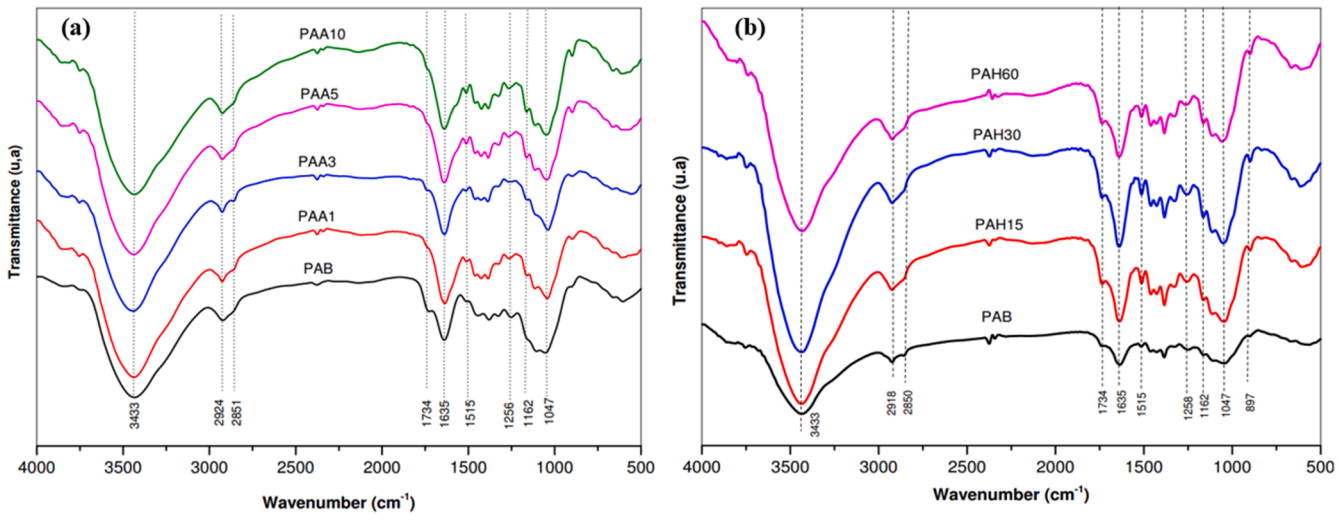

Fig. 5. FTIR spectrum of raw *PAB* and treated *PA* fibers: alkaline (a); hydrothermal (b).

Table 2
Band positions and functional group assignments in raw and NaOH treated *PA* fibers based on literature (El Achaby et al., 2018; Maache et al., 2017; Ramkumar & Saravanan, 2021; Reddy et al., 2014; Saravanakumar et al., 2013).

Wave number (cm^{-1})					Assignments
PAB	*PAA1*	*PAA3*	*PAA5*	*PAA10*	
3433	3446	3443	3442	3445	O-H stretching (cellulose & hemicellulose)
2924	2925	2924	2923	2923	C-H stretching of alkyls (cellulose & hemicellulose)
2851	2857	2861	2856	2858	CH2 Symmetric stretching (cellulose & hemicellulose)
1734	-	-	-	-	Stretching of the C=O of the hemicellulose
1635	1650	1640	1643	1646	Stretching of the C-O of lignin
1515	1513	1515	1512	1515	Stretching of the C-O of lignin
1162	1164	1162	1162	1164	Asymmetric C-O-C stretching (cellulose and hemicellulose)
1047	1039	1056	1053	1056	Symmetrical stretching of the C-O of lignin
897	899	894	897	897	C-H bonding of the aromatic hydrogen of a lignin compound

Table 3
Band positions and functional group assignments in raw and boil-treated *PA* fibers, based on literature (El Achaby et al., 2018; Maache et al., 2017; Ramkumar & Saravanan, 2021; Reddy et al., 2014; Saravanakumar et al., 2013).

Wave number (cm^{-1})				Assignments
PAB	*PAH15*	*PAH30*	*PAH60*	
3433	3433	3432	3432	O-H stretching (cellulose & hemicellulose)
2918	2918	2918	2920	C-H stretching of alkyls (cellulose & hemicellulose)
2850	2852	2854	2852	CH2 Symmetric stretching (cellulose & hemicellulose)
1734	-	-	-	Stretching of the C=O of the hemicellulose
1635	1632	1634	1635	Stretching of the C-O of lignin
1515	1513	1512	1512	Stretching of the C-O of lignin
1162	1164	1162	1162	Asymmetric C-O-C stretching (cellulose and hemicellulose)
1047	1042	1045	1048	Symmetrical stretching of the C-O of lignin
897	898	895	896	C-H bonding of the aromatic hydrogen of a lignin compound

fiber degradation at this concentration (Achour et al., 2017; Ajouguim et al., 2019). Figs. 6b and 8 show the X-ray spectra of boiling water-treated fibers and the evolution of the crystallinity of these fibers as a function of treatment time. The results of this study show an increase in crystallinity index up to 55.24 for 60 min. The increase in the crystallinity index is attributed to the removal of amorphous components from the fiber. Climatic conditions affect not only the fiber structure but also its composition (Mouhoubi et al., 2017). A lower hemicellulose content is desirable, as a higher content degrades thermal stability and increases moisture absorption capacity (Azwa et al., 2013). On the other hand, lignin improves fiber stiffness by binding the cell wall structures together. It also contributes to polymer bonding when used as reinforcement in polymer matrix composites (Beaugrand et al., 2014; Jawaid & Khalil, 2011).

3.4.3. *Evolution of the crystallinity index*

Using the Scherer equation, the crystallite size (L) of *Pennisetum alopecuroides* fibers calculated is 0.49 nm, which is significantly smaller than that determined for *flax* (2.8 nm), *corn* (3.8 nm), and *cotton* (5.5 nm) fibers, and quite close to *coir* (0.43 nm) (Dharmaratne et al., 2021; Indran et al., 2014). Smaller crystal size structures tend to absorb more water than higher crystal size structures (Indran et al., 2014).

3.5. *Thermal analysis*

The TGA and DTG curves of the *Pennisetum alopecuroides* fiber are presented in Fig. 9. The decomposition of the different components of the *PA* fiber is done in three steps. The first weight loss at temperatures below 100°C corresponds to the loss of water and removal of waxy material from the fibers (Maache et al., 2017; Manimaran et al., 2020). The second weight loss at 290°C related to the decomposition of hemicellulose and the glycosidic bonds of cellulose (Balaji & Nagarajan, 2017; Belouadah et al., 2015).

A significant weight loss (70 wt%) was found at 337°C. This could be attributed to the decomposition of cellulose I, α cellulose, and lignin (Balaji & Nagarajan, 2017; Fiore et al., 2014; Manimaran et al., 2018; Saravanakumar et al., 2013). However, lignin, due to the presence of phenyl groups, is the most difficult to decompose and its decomposition extends over the entire temperature range from below 200°C to 700°C (Reddy et al., 2009; Yang et al., 2007). Moreover, the degradation temperature of *PA* is relatively similar to that of *Okra* (220°C), *Hemp* (250°C), *Curaua* (230°C), *Kenaf* (219°C), *Jute* (205°C) (De Rosa et al., 2011).

3.6. *Morphological analysis by EDX*

3.6.1. *Raw fibers*

Fig. 10a presents the EDX spectrum for the raw *PA* fiber. The fiber is

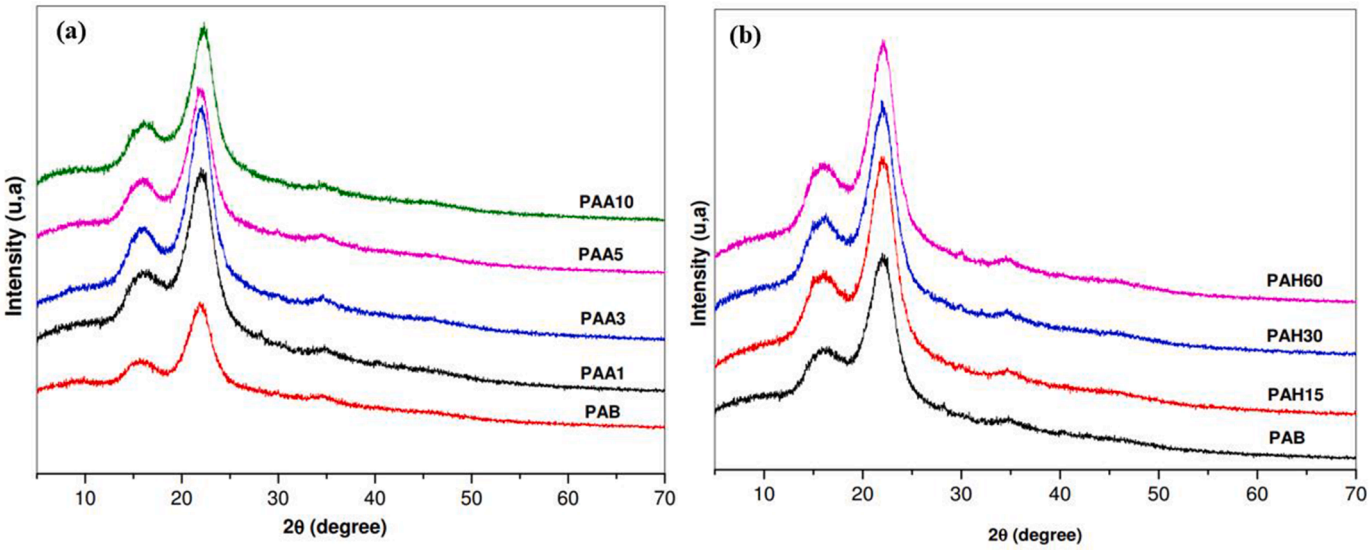

Fig. 6. X-ray diffractograms of raw *PA* fibers and treated: alkaline (a); hydrothermal (b).

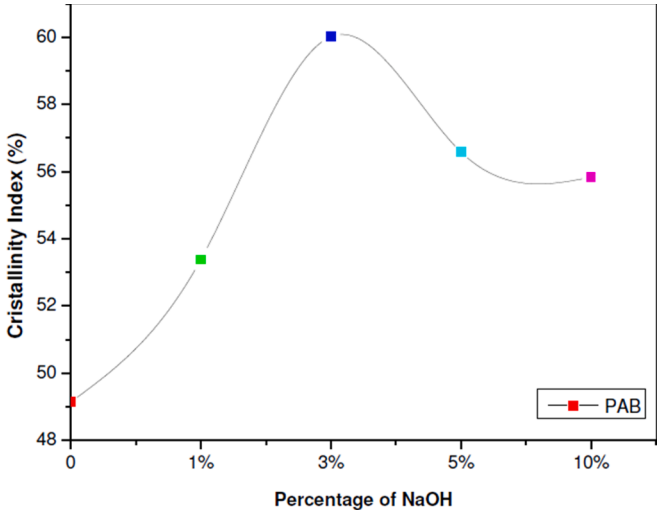

Fig. 7. Evolution of the crystallinity index of *PA* fibers as a function of alkaline treatment.

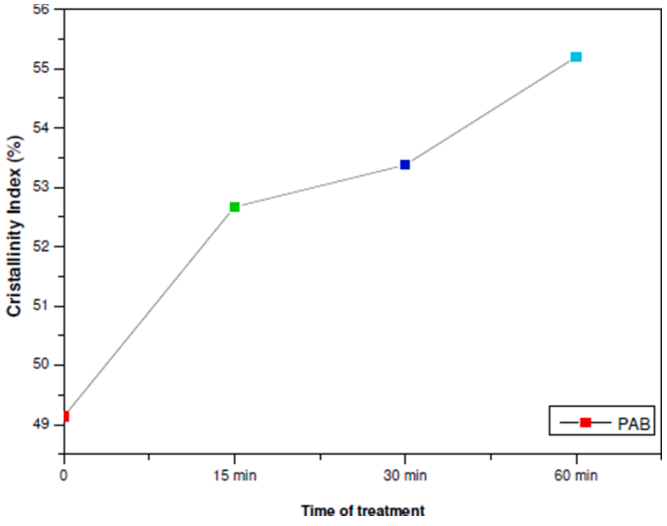

Fig. 8. Evolution of the crystallinity index of *PA* fibers as a function of the duration of boiling water treatment.

composed of elements such as carbon (C), oxygen (O), a small amount of silicon (Si), and traces of chlorine (Cl), potassium (K), calcium (Ca), and aluminum (Al).

Based on the results in Table 4, which show the mass and atomic percentage calculated from the peak areas, carbon and oxygen are the main constituents as they are the majority components found in natural fiber structures (Kambli et al., 2016). This is consistent with the known chemical composition of lignocellulosic fibers. The mass percentage revealed that *P. alopecuroides* fiber contains less carbon (47.95 wt%) than *jute* fiber (55.68 wt%) and *Vascular bundles* fiber (50.14 wt%) (Boumediri et al., 2019; Moshi et al., 2020). But it has a non-negligible content of silicon (5.56 wt%) and traces of potassium (1.72 wt%), sulfur (0.68 wt%), calcium (0.46 wt%), and aluminum (0.23 wt%) compared to other natural fibers.

3.6.2. *Treated fibers*

Fig. 11 compares the surface of the untreated and chemically treated fibers. The surface of the untreated fiber (Fig. 11a) shows impurities. The micrographs (Fig. 11b, c, d) indicate that the hydrothermal treatment has removed some of the impurities.

The micrographs (Fig. 11e, f, g, h) indicate that the alkaline treatment improved the surface morphology of the fibers. The NaOH treatment acts on the middle lamella and the secondary wall leading to the removal of hemicelluloses and the dissolution of pectins, but as soon as the concentration exceeds 3% the degradation of the cell wall can be noticed due to the excessive extraction of hemicellulose and lignin.

4. Conclusions

In this work, the effect of hydrothermal and alkaline treatments on *Pennisetum alopecuroides (PA)* fibers were analyzed for the first time. For the hydrothermal treatment the effect of the duration of immersion in boiling water at 100°C temperature was assessed (15 min, 30 min and 60 min). For the alkaline treatment the effect of the NaOH concentrations (1%, 3%, 5%, and 10%) was evaluated.

The physicochemical, morphological, and thermogravimetric characterization was performed for untreated and treated *PA* fibers. The following conclusions can be drawn:

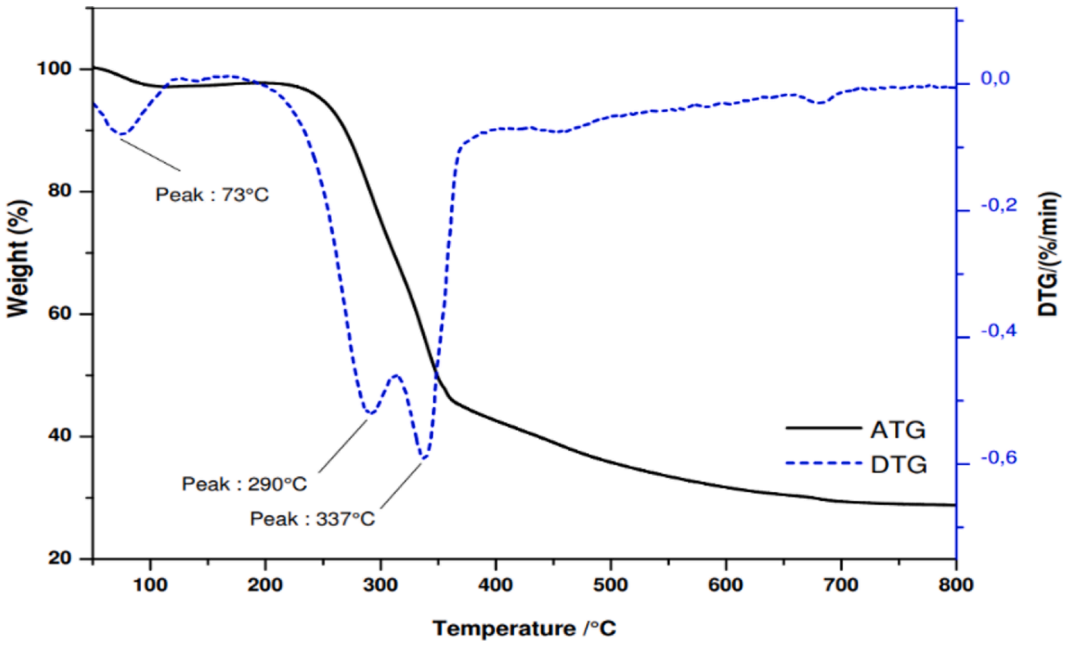

Fig. 9. TGA and DTG curves of raw *PA* fibers.

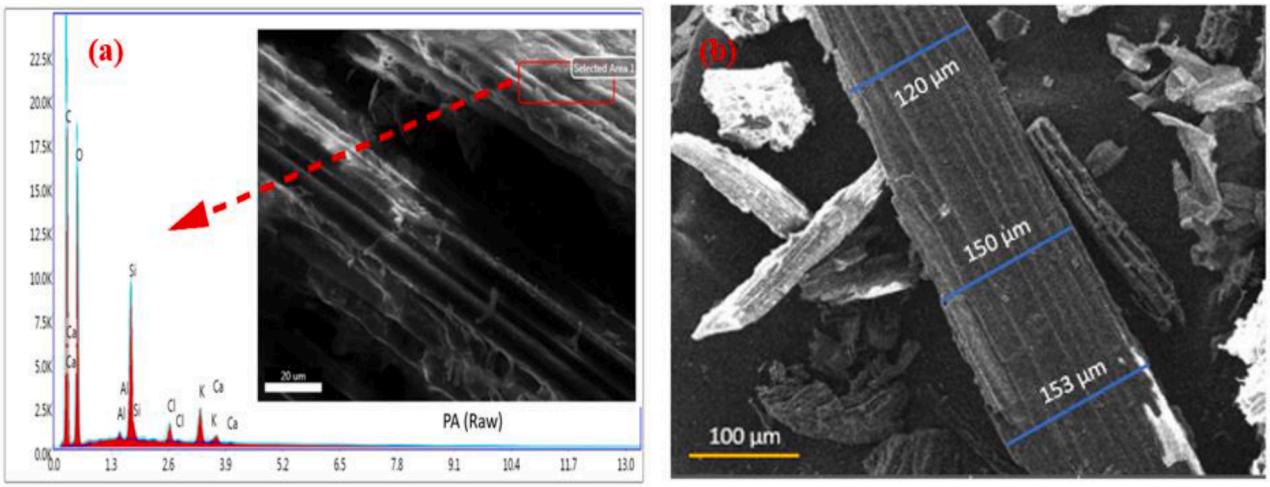

Fig. 10. (a) EDX analysis of the raw *PA* fiber (b) Diameter measurement through SEM images.

Table 4
Mass and atomic percentage of raw *PA* fiber and other natural fibers.

Elements	*PA* (raw)		*Vascular bundles* (Boumediri et al., 2019)		*Coccinia Grandis* (Moshi et al., 2020)		*Jute* (Moshi et al., 2020)	
	Weight	Atomic	Weight	Atomic	Weight	Atomic	Weight	Atomic
	(%)	(%)	(%)	(%)	(%)	(%)	(%)	(%)
C	47.95	56.93	50.14	57.88	44.67	51.91	55.68	62.72
O	44.40	39.57	46.41	40.22	54.38	47.58	43.89	37.11
Si	4.56	2.32	0.47	0.23	0.67	0.36	0.11	0.06
K	1.72	0.63	0.06	0.02	-	-	-	-
Cl	0.68	0.27	0.14	0.06	0.38	0.06	-	-
Ca	0.46	0.16	0.05	0.02	-	-	-	-
Al	0.23	0.12	0.86	0.44	0.18	0.09	-	-

- The chemical analysis shows that the *PA* fibers have cellulose, hemicellulose, and lignin content in the order of 49 wt%, 30% and 20% respectively, and these values are comparable to other lignocellulosic fibers reported in the literature.
- The density of the *PA* fibers (870 kg/m^3) presents a lower value compared to other cellulosic fibers, namely *jute* fiber (1460 kg/m^3), and synthetic fibers, such as glass fiber (2500 kg/m^3).
- The FTIR analysis indicates a decrease in hemicellulose and lignin content due to the alkaline and hydrothermal treatments.

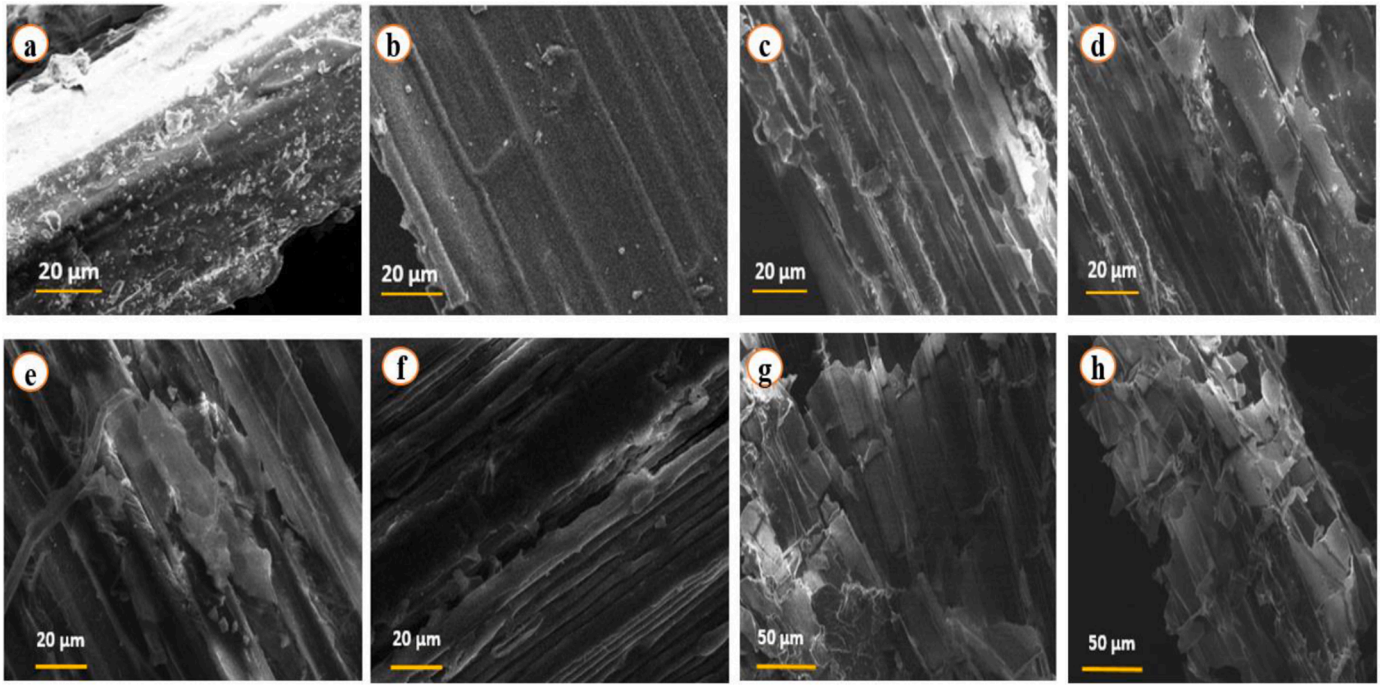

Fig. 11. SEM micrographs of *PA* fiber after hydrothermal (*PAH*) and alkaline (*PAA*) treatment: (a) untreated (*BAP*), (b) *PAH15*, (c) *PAH30*, (d) *PAH60*, (e) *PAA1*, (f) *PAA3*, (g) *PAA5*, (h) *PAA10*.

- XRD analysis shows that the crystallinity index of the *PA* fibers increases after alkaline (60%) and hydrothermal (55%) treatments.
- The results of the thermo-gravimetric analysis reveals that the *PA* fibers were thermally stable up to 226°C, which is much higher than the temperature of polymerization process.
- The SEM micrograph reveals a smoother surface morphology for the untreated *PA* rods. The 3% NaOH alkaline and 60 min hydrothermal treatments are optimal for this fiber, since they remove the amorphous components and the surface becomes rough, leading to most probable good interfacial adhesion of the fiber with a matrix, in case it is used to produce composites.
- The EDX analysis confirms that carbon and oxygen are the main constituents of the *PA* fiber, which means that the fiber keeps its organic nature.

Finally, the characterization of the treated *PA* fibers shows results which seem to validate a promising use of those fibers for various industrial applications. Therefore, the use of the *PA* fibers for production of composites for the construction industry, such as insulation boards contributing for building energy efficiency, is suggested for future work.

Declaration of Competing Interest

There is no conflict of interest.

Data availability

Data will be made available on request.

Acknowledgments

The authors would express their sincere thanks to the Moroccan Center for Analysis and Characterization (CAC) affiliated to Cadi Ayyad University, for providing some sample characterizations.

References

Achour, A., Ghomari, F., & Belayachi, N. (2017). Properties of cementitious mortars reinforced with natural fibers. *Journal of Adhesion Science and Technology, 31*(17), 1938–1962.

Ahmed, M. J., Balaji, M. S., Saravanakumar, S. S., Sanjay, M. R., & Senthamaraikannan, P. (2019). Characterization of Areva javanica fiber–A possible replacement for synthetic acrylic fiber in the disc brake pad. *Journal of Industrial Textiles, 49*(3), 294–317.

Ajouguim, S., Abdelouahdi, K., Waqif, M., Stefanidou, M., & Saâdi, L. (2019). Modifications of Alfa fibers by alkali and hydrothermal treatment. *Cellulose, 26*(3), 1503–1516.

Ariawan, D., Rivai, T. S., Surojo, E., Hidayatulloh, S., Akbar, H. I., & Prabowo, A. R. (2020). Effect of alkali treatment of Salacca Zalacca fiber (SZF) on mechanical properties of HDPE composite reinforced with SZF. *Alexandria Engineering Journal, 59*(5), 3981–3989.

Arthanarieswaran, V. P., Kumaravel, A., & Saravanakumar, S. S. (2015). Characterization of new natural cellulosic fiber from Acacia leucophloea bark. *International Journal of Polymer Analysis and Characterization, 20*(4), 367–376.

Azwa, Z. N., Yousif, B. F., Manalo, A. C., & Karunasena, W. (2013). A review on the degradability of polymeric composites based on natural fibres. *Materials & Design, 47*, 424–442.

Balaji, A. N., & Nagarajan, K. J. (2017). Characterization of alkali treated and untreated new cellulosic fiber from Saharan aloe vera cactus leaves. *Carbohydrate Polymers, 174*, 200–208.

Balasundar, P., Narayanasamy, P., Senthamaraikannan, P., Senthil, S., Prithivirajan, R., & Ramkumar, T. (2018a). Extraction and characterization of new natural cellulosic chloris barbata fiber. *Journal of Natural Fibers, 15*(3), 436–444.

Balasundar, P., Narayanasamy, P., Senthamaraikannan, P., Senthil, S., Prithivirajan, R., & Ramkumar, T. (2018b). Extraction and characterization of new natural cellulosic chloris barbata fiber. *Journal of Natural Fibers, 15*(3), 436–444.

Beaugrand, J., Nottez, M., Konnerth, J., & Bourmaud, A. (2014). Multi-scale analysis of the structure and mechanical performance of woody hemp core and the dependence on the sampling location. *Industrial Crops and Products, 60*, 193–204.

Belouadah, Z., Ati, A., & Rokbi, M. (2015). Characterization of new natural cellulosic fiber from Lygeum spartum L. *Carbohydrate Polymers, 134*, 429–437.

Bezazi, A., Belaadi, A., Bourchak, M., Scarpa, F., & Boba, K. (2014). Novel extraction techniques, chemical and mechanical characterisation of Agave americana L. natural fibres. *Composites Part B: Engineering, 66*, 194–203.

Boopathi, L., Sampath, P. S., & Mylsamy, K. (2012). Investigation of physical, chemical and mechanical properties of raw and alkali treated Borassus fruit fiber. *Composites Part B: Engineering, 43*(8), 3044–3052.

Boumediri, H., Bezazi, A., Del Pino, G. G., Haddad, A., Scarpa, F., & Dufresne, A. (2019). Extraction and characterization of vascular bundle and fiber strand from date palm rachis as potential bio-reinforcement in composite. *Carbohydrate Polymers, 222*, Article 114997.

Cai, M., Takagi, H., Nakagaito, A. N., Katoh, M., Ueki, T., Waterhouse, G. I., & Li, Y. (2015). Influence of alkali treatment on internal microstructure and tensile properties of abaca fibers. *Industrial Crops and Products, 65*, 27–35.
Chakravarthy, S., Madhu, S., Raju, J. S. N., & Md, J. S. (2020). Characterization of novel natural cellulosic fiber extracted from the stem of cissus vitiginea plant. *International Journal of Biological Macromolecules, 161*, 1358–1370.
Cintura, E., Faria, P., Duarte, M., & Nunes, L. (2022). Bio-wastes as aggregates for eco-efficient boards and panels: screening tests of physical properties and bio-susceptibility. *Infrastructures, 7*(3), 26.
de-Andrade-Silva, F., Chawla, N., & de Toledo Filho, R. D. (2008). Tensile behavior of high performance natural (sisal) fibers. *Composites Science and Technology, 68*(15), 3438–3443. –16.
De-Rosa, I. M., Kenny, J. M., Maniruzzaman, M., Moniruzzaman, M., Monti, M., Puglia, D., Santulli, C., & Sarasini, F. (2011). Effect of chemical treatments on the mechanical and thermal behaviour of okra (Abelmoschus esculentus) fibres. *Composites Science and Technology, 71*(2), 246–254.
Dharmaratne, P. D., Galabada, H., Jayasinghe, R., Nilmini, R., & Halwatura, R. U. (2021). Characterization of physical, chemical and mechanical properties of Sri Lankan coir fibers. *Journal of Ecological Engineering*, (6), 22.
El-Achaby, M., Kassab, Z., Barakat, A., & Aboulkas, A. (2018). Alfa fibers as viable sustainable source for cellulose nanocrystals extraction: Application for improving the tensile properties of biopolymer nanocomposite films. *Industrial Crops and Products, 112*, 499–510.
El-Omari, H., Belfkira, A., & Brouillette, F. (2017). Paper properties of Typha Latifolia, Pennisetum Alopecuroides, and Agave Americana fibers and their effect as a substitute for kraft pulp fibers. *Journal of Natural Fibers, 14*(3), 426–436. https://doi.org/10.1080/15440478.2016.1212766
Elanthikkal, S., Gopalakrishnapanicker, U., Varghese, S., & Guthrie, J. T. (2010). Cellulose microfibres produced from banana plant wastes: Isolation and characterization. *Carbohydrate Polymers, 80*(3), 852–859.
Faruk, O., Bledzki, A. K., Fink, H.-P., & Sain, M. (2012). Biocomposites reinforced with natural fibers: 2000–2010. *Progress in Polymer Science, 37*(11), 1552–1596.
Ferreira, S. R., de Andrade Silva, F., Lima, P. R. L., & Toledo Filho, R. D. (2015). Effect of fiber treatments on the sisal fiber properties and fiber–matrix bond in cement based systems. *Construction and Building Materials, 101*, 730–740.
Fiore, V., Scalici, T., & Valenza, A. (2014). Characterization of a new natural fiber from Arundo donax L. as potential reinforcement of polymer composites. *Carbohydrate Polymers, 106*, 77–83.
French, A. D., & Santiago Cintrón, M. (2013). Cellulose polymorphy, crystallite size, and the Segal Crystallinity Index. *Cellulose, 20*(1), 583–588.
Gurukarthik-Babu, B., Prince-Winston, D., SenthamaraiKannan, P., Saravanakumar, S. S., & Sanjay, M. R (2019). Study on characterization and physicochemical properties of new natural fiber from Phaseolus vulgaris. *Journal of Natural Fibers, 16*(7), 1035–1042.
Hernandez, C. C., Ferreira, F. F., & Rosa, D. S. (2018). X-ray powder diffraction and other analyses of cellulose nanocrystals obtained from corn straw by chemical treatments. *Carbohydrate Polymers, 193*, 39–44.
Ibrahim, M. M., Agblevor, F. A., & El-Zawawy, W. K. (2010). Isolation and characterization of cellulose and lignin from steam-exploded lignocellulosic biomass. *BioResources, 5*(1), 397–418.
Indran, S., & Raj, R. E. (2015). Characterization of new natural cellulosic fiber from Cissus quadrangularis stem. *Carbohydrate Polymers, 117*, 392–399.
Indran, S., Raj, R. E., & Sreenivasan, V. S. (2014). Characterization of new natural cellulosic fiber from Cissus quadrangularis root. *Carbohydrate Polymers, 110*, 423–429.
Jawaid, M., & Khalil, H. A. (2011). Cellulosic/synthetic fibre reinforced polymer hybrid composites: A review. *Carbohydrate Polymers, 86*(1), 1–18.
Jayaramudu, J., Guduri, B. R., & Rajulu, A. V. (2010). Characterization of new natural cellulosic fabric Grewia tilifolia. *Carbohydrate Polymers, 79*(4), 847–851.
Kamaruddin, Z. H., Jumaidin, R., Rushdan, A. I., Selamat, M. Z., & Alamjuri, R. H. (2021). Characterization of natural cellulosic fiber isolated from malaysian cymbopogan citratus leaves. *BioResources, 16*(4).
Kambli, N., Basak, S., Samanta, K. K., & Deshmukh, R. R. (2016). Extraction of natural cellulosic fibers from cornhusk and its physico-chemical properties. *Fibers and Polymers, 17*(5), 687–694.
Kathirselvam, M., Kumaravel, A., Arthanarieswaran, V. P., & Saravanakumar, S. S. (2019). Isolation and characterization of cellulose fibers from Thespesia populnea barks: A study on physicochemical and structural properties. *International Journal of Biological Macromolecules, 129*, 396–406.
Khan, A., Vijay, R., Singaravelu, D. L., Sanjay, M. R., Siengchin, S., Jawaid, M., Alamry, K. A., & Asiri, A. M. (2022). Extraction and characterization of natural fibers from Citrullus lanatus climber. *Journal of Natural Fibers, 19*(2), 621–629.
Khoudja, D., Taallah, B., Izemmouren, O., Aggoun, S., Herihiri, O., & Guettala, A. (2021). Mechanical and thermophysical properties of raw earth bricks incorporating date palm waste. *Construction and Building Materials, 270*, Article 121824.
Ko, J. O., Kim, S. K., Lim, Y. R., Han, J. K., Yoon, Y., Ji, S., Lee, M., Kim, S.-W., Song, W., & Myung, S. (2019). Foldable and water-resist electrodes based on carbon nanotubes/methyl cellulose hybrid conducting papers. *Composites Part B: Engineering, 160*, 512–518.
Lau, K., Hung, P., Zhu, M.-H., & Hui, D. (2018). Properties of natural fibre composites for structural engineering applications. *Composites Part B: Engineering, 136*, 222–233.
Maache, M., Bezazi, A., Amroune, S., Scarpa, F., & Dufresne, A. (2017). Characterization of a novel natural cellulosic fiber from Juncus effusus L. *Carbohydrate Polymers, 171*, 163–172.
Maheshwaran, M. V., Hyness, N. R. J., Senthamaraikannan, P., Saravanakumar, S. S., & Sanjay, M. R. (2018). Characterization of natural cellulosic fiber from Epipremnum aureum stem. *Journal of Natural Fibers, 15*(6), 789–798.
Manimaran, P., Pillai, G. P., Vignesh, V., & Prithiviraj, M. (2020). Characterization of natural cellulosic fibers from Nendran Banana Peduncle plants. *International Journal of Biological Macromolecules, 162*, 1807–1815.
Manimaran, P., Saravanan, S. P., Sanjay, M. R., Siengchin, S., Jawaid, M., & Khan, A. (2019). Characterization of new cellulosic fiber: Dracaena reflexa as a reinforcement for polymer composite structures. *Journal of Materials Research and Technology, 8*(2), 1952–1963.
Manimaran, P., Senthamaraikannan, P., Sanjay, M. R., Marichelvam, M. K., & Jawaid, M. (2018). Study on characterization of Furcraea foetida new natural fiber as composite reinforcement for lightweight applications. *Carbohydrate Polymers, 181*, 650–658.
Moosavinejad, S. M., Madhoushi, M., Vakili, M., & Rasouli, D. (2019). Evaluation of degradation in chemical compounds of wood in historical buildings using FT-IR and FT-Raman vibrational spectroscopy. *Maderas Ciencia y Tecnología, 21*(3), 381–392.
Morán, J. I., Alvarez, V. A., Cyras, V. P., & Vázquez, A. (2008). Extraction of cellulose and preparation of nanocellulose from sisal fibers. *Cellulose, 15*(1), 149–159.
Moshi, A. A. M., Ravindran, D., Bharathi, S. S., Indran, S., Saravanakumar, S. S., & Liu, Y. (2020). Characterization of a new cellulosic natural fiber extracted from the root of Ficus religiosa tree. *International Journal of Biological Macromolecules, 142*, 212–221.
Mouhoubi, S., Bourahli, M. E. H., Osmani, H., & Abdeslam, S. (2017). Effect of alkali treatment on alfa fibers behavior. *Journal of Natural Fibers, 14*(2), 239–249.
Msahli, S., Jaouadi, M., Sakli, F., & Drean, J.-Y. (2015). Study of the mechanical properties of fibers extracted from Tunisian Agave americana L. *Journal of Natural Fibers, 12*(6), 552–560.
Naili, H., Jelidi, A., Limam, O., & Khiari, R. (2017). Extraction process optimization of Juncus plant fibers for its use in a green composite. *Industrial Crops and Products, 107*, 172–183.
Nunes, L., Cintura, E., Parracha, J. L., Fernandes, B., Silva, V., & Faria, P. (2021). Cement-bonded particleboards with banana pseudostem waste: Physical performance and bio-susceptibility. *Infrastructures, 6*(6), 86.
Omrani, H., Hassini, L., Benazzouk, A., Beji, H., & ELCafsi, A. (2020). Elaboration and characterization of clay-sand composite based on Juncus acutus fibers. *Construction and Building Materials, 238*, Article 117712.
Pandiarajan, P., Kathiresan, M., Baskaran, P. G., & Kanth, J. (2022). Characterization of raw and alkali treated new cellulosic fiber from the rinds of Thespesia populnea plant. *Journal of Natural Fibers, 19*(11), 4038–4049.
Prado, K. S., & Spinacé, M. A. (2019). Isolation and characterization of cellulose nanocrystals from pineapple crown waste and their potential uses. *International Journal of Biological Macromolecules, 122*, 410–416.
Prithiviraj, M., Muralikannan, R., Senthamaraikannan, P., & Saravanakumar, S. S. (2016). Characterization of new natural cellulosic fiber from the Perotis indica plant. *International Journal of Polymer Analysis and Characterization, 21*(8), 669–674.
Ramkumar, R., & Saravanan, P. (2021). Characterization of the cellulose fibers extracted from the bark of Piliostigma Racemosa. *Journal of Natural Fibers*, 1–15.
Ravindran, D., SR, S. B., & Indran, S. (2020). Characterization of surface-modified natural cellulosic fiber extracted from the root of Ficus religiosa tree. *International Journal of Biological Macromolecules, 156*, 997–1006.
Reddy, K. O., Ashok, B., Reddy, K. R. N., Feng, Y. E., Zhang, J., & Rajulu, A. V. (2014). Extraction and characterization of novel lignocellulosic fibers from Thespesia lampas plant. *International Journal of Polymer Analysis and Characterization, 19*(1), 48–61.
Reddy, K. O., Maheswari, C. U., Reddy, D. J. P., & Rajulu, A. V. (2009). Thermal properties of Napier grass fibers. *Materials Letters, 63*(27), 2390–2392.
Ridzuan, M. J. M., Majid, M. A., Afendi, M., Kanafiah, S. A., Zahri, J. M., & Gibson, A. G. (2016). Characterisation of natural cellulosic fibre from Pennisetum purpureum stem as potential reinforcement of polymer composites. *Materials & Design, 89*, 839–847.
Sanjay, M. R., Madhu, P., Jawaid, M., Senthamaraikannan, P., Senthil, S., & Pradeep, S. (2018). Characterization and properties of natural fiber polymer composites: A comprehensive review. *Journal of Cleaner Production, 172*, 566–581.
Saravanakumar, S. S., Kumaravel, A., Nagarajan, T., Sudhakar, P., & Baskaran, R. (2013). Characterization of a novel natural cellulosic fiber from Prosopis juliflora bark. *Carbohydrate Polymers, 92*(2), 1928–1933.
Sathishkumar, T. P., Navaneethakrishnan, P., Shankar, S., & Rajasekar, R. (2013). Characterization of new cellulose sansevieria ehrenbergii fibers for polymer composites. *Composite Interfaces, 20*(8), 575–593.
Segal, L., Creely, J. J., Martin-Jr, A. E., & Conrad, C. M (1959). An empirical method for estimating the degree of crystallinity of native cellulose using the X-ray diffractometer. *Textile Research Journal, 29*(10), 786–794.
Senthamaraikannan, P., & Kathiresan, M. (2018). Characterization of raw and alkali treated new natural cellulosic fiber from Coccinia grandis. L. *Carbohydrate Polymers, 186*, 332–343.
Senthamaraikannan, P., Saravanakumar, S. S., Sanjay, M. R., Jawaid, M., & Siengchin, S. (2019). Physico-chemical and thermal properties of untreated and treated Acacia planifrons bark fibers for composite reinforcement. *Materials Letters, 240*, 221–224. https://doi.org/10.1016/j.matlet.2019.01.024
Singh, G., Jose, S., Kaur, D., & Soun, B. (2022). Extraction and characterization of corn leaf fiber. *Journal of Natural Fibers, 19*(5), 1581–1591.
Umashankaran, M., & Gopalakrishnan, S. (2021). Effect of sodium hydroxide treatment on physico-chemical, thermal, tensile and surface morphological properties of pongamia Pinnata L. bark fiber. *Journal of Natural Fibers, 18*(12), 2063–2076.
Vijay, R., Vinod, A., Singaravelu, D. L., Sanjay, M. R., & Siengchin, S. (2021). Characterization of chemical treated and untreated natural fibers from Pennisetum orientale grass-A potential reinforcement for lightweight polymeric applications. *International Journal of Lightweight Materials and Manufacture, 4*(1), 43–49.

Vinod, A., Vijay, R., Singaravelu, D. L., Sanjay, M. R., Siengchin, S., Yagnaraj, Y., & Khan, S. (2021). Extraction and characterization of natural fiber from stem of cardiospermum halicababum. *Journal of Natural Fibers, 18*(6), 898–908.
Yang, H., Yan, R., Chen, H., Lee, D. H., & Zheng, C. (2007). Characteristics of hemicellulose, cellulose and lignin pyrolysis. *Fuel, 86*(12), 1781–1788. –13.
Zhou, L., Shao, J.-Z., Feng, X.-X., & Chen, J.-Y. (2012). Effect of high-temperature degumming on the constituents and structure of cotton stalk bark fibers. *Journal of Applied Polymer Science, 125*(S2), E573–E579.